NO_y partitioning and aerosol influences in the stratosphere

V. Küll,[1] M. Riese,[1,2] X. Tie,[3] T. Wiemert,[1,4] G. Eidmann,[1,5] D. Offermann,[1] and G. P. Brasseur[6]

Received 23 August 2001; revised 4 March 2002; accepted 5 March 2002; published 24 October 2002.

[1] The Cryogenic Infrared Spectrometers and Telescopes for the Atmosphere (CRISTA) instrument measured a variety of trace gases globally with high spatial resolution during two Space Shuttle missions. This paper concentrates on members of the NO_y family and highlights differences between CRISTA 1 (November 1994) and CRISTA 2 (August 1997). A sequential assimilation technique is used to combine the CRISTA measurements of total NO_y fields with corresponding model forecasts based on the National Center for Atmospheric Research Research for Ozone in the Stratosphere and its Evolution (ROSE) model. For this study we use a model version driven by wind and temperature data provided by the UK Met Office. NO_2 and N_2O show large- and medium-scale structures caused by dynamical processes. N_2O_5 shows a strong dependence on the aerosol load and solar zenith angles. N_2O_5 and NO_2 changes from CRISTA 1 to CRISTA 2 are consistent with a reduction of aerosol concentrations in the Southern Hemisphere and minor aerosol changes in the Northern Hemisphere. For both missions the model reproduces well the measured diurnal cycles of the NO_y family members. Measured diurnal variations of N_2O_5 and NO_2 are consistent with the nighttime production of N_2O_5 from NO_2. Compared to the effect of heterogeneous chemistry, the influence of ozone and temperature changes on the NO_y partitioning is rather small. A model run based on a three-dimensional aerosol field derived from CRISTA observations indicates that zonal asymmetries in the background aerosol have strong local effects on the N_2O_5 and NO_2 distribution. *INDEX TERMS:* 0341 Atmospheric Composition and Structure: Middle atmosphere—constituent transport and chemistry (3334); 3337 Meteorology and Atmospheric Dynamics: Numerical modeling and data assimilation; 0933 Exploration Geophysics: Remote sensing; *KEYWORDS:* stratosphere, NO_y, three-dimensional, aerosol, chemistry, data assimilation

Citation: Küll, V., M. Riese, X. Tie, T. Wiemert, G. Eidmann, D. Offermann, and G. Brasseur, NO_y partitioning and aerosol influences in the stratosphere, *J. Geophys. Res.*, *107*(D23), 8183, doi:10.1029/2001JD001246, 2002.

1. Introduction

[2] The members of the NO_y family (NO_y = N + NO + NO_2 + NO_3 + 2 N_2O_5 + HNO_3 + HO_2NO_2 + $ClONO_2$ + $BrONO_2$) play a crucial role in stratospheric chemistry. NO_x (= NO + NO_2), as its most reactive form, is responsible for up to 70% of stratospheric ozone loss [*Portmann et al.*, 1999]. NO_x reactions dominate the catalytic destruction of ozone between 25 and 40 km altitude [*Crutzen*, 1970; *Johnston*, 1971]:

(R1) $$NO + O_3 \rightarrow NO_2 + O_2$$

(R2) $$NO_2 + O \rightarrow NO + O_2 \qquad \text{(rate limiting step)}$$

[3] Reaction (1) and the NO_2 photolysis account for more than 90% of the NO_x chemistry in the lower stratosphere [*Del Negro et al.*, 1999; *Cohen et al.*, 2000]. Although NO_x can directly destroy ozone, it can also buffer ozone-destroying chlorine compounds, mainly by reaction (3):

(R3) $$NO_2 + ClO + M \rightarrow ClONO_2 + M$$

[4] The partitioning of NO_y into reactive and reservoir species and the interchanging reactions are therefore of major interest. During daytime, NO_2 is converted to the reservoir gas HNO_3 by the gas-phase reaction (4):

(R4) $$NO_2 + OH + M \rightarrow HNO_3 + M$$

The recovery of NO_2 is facilitated by reaction (5):

(R5) $$HNO_3 + OH \rightarrow NO_3 + H_2O$$

[5] In addition, NO_x is created by thermal decomposition of N_2O_5 and by photolysis of the NO_y reservoirs (in particular by photolysis of HNO_3).

[1]Physics Department, University of Wuppertal, Germany.
[2]Now at Institute for Stratospheric Research, Juelich Research Center, Juelich, Germany.
[3]National Center for Atmospheric Research, Boulder, Colorado, USA.
[4]Now at T-Systems GEI GmbH, Aachen, Germany.
[5]Now at Vacuumschmelze GmbH & Co. KG, Hanau, Germany.
[6]Max Planck Institute for Meteorology, Hamburg, Germany.

0148-0227/02/2001JD001246

[6] An important channel from reactive nitrogen to reservoir species is the formation of N_2O_5 followed by the heterogeneous reaction on aqueous aerosol (hydrolysis) to HNO_3 by reactions (6) through (8):

(R6) $$NO_2 + O_3 \rightarrow NO_3 + O_2$$

(R7) $$NO_3 + NO_2 + M \rightarrow N_2O_5 + M$$

(R8) $$N_2O_5 + H_2O(aq) \rightarrow 2\ HNO_3$$

[7] These reactions occur mostly at night, when the intermediate products N_2O_5 and NO_3 are not photolyzed.

[8] The N_2O_5 molecule is an important intermediate product in the reaction chain (6)–(8). Since N_2O_5 is directly influenced by heterogeneous chemistry (reaction (8)), the NO_y partitioning depends on the aerosol load, which is influenced to a large extent by major volcanic eruptions. The eruption of Mount Pinatubo in June 1991, which caused the greatest stratospheric aerosol load in the 20th century [*McCormick et al.*, 1995], demonstrated the strong dependence of the NO_x/NO_y partitioning on the aerosol load [*Fahey et al.*, 1993]. The response of the nitrogen chemistry has been subject to a number of analyses utilizing data from ground-based [e.g., *Koike et al.*, 1994], balloonborne [e.g., *Webster et al.*, 1994; *Sen et al.*, 1998], airborne [e.g., *Fahey et al.*, 1993] and satellite experiments [e.g., *Rinsland et al.*, 1994; *Kinnison et al.*, 1994; *Morris et al.*, 1997; *Danilin et al.*, 1999] as well as model studies [e.g., *Brasseur and Granier*, 1992; *Bekki and Pyle*, 1994; *Tie et al.*, 1994]. Data from the Stratospheric Aerosol and Gas Experiment II (SAGE II) [*Thomason et al.*, 1997] shows a fast recovery of the lower stratosphere from the Mount Pinatubo aerosol load until 1994, followed by a flat transition to background levels in 1997 [*Randel et al.*, 1999].

[9] The two CRISTA flights took place during both the declining period of the aerosol load (CRISTA 1, November 1994) and the transition to aerosol background conditions (CRISTA 2, August 1997). *Perkins et al.* [2001], *Cohen et al.* [2000], and *Osterman et al.* [1999] employed balloonborne and aircraftborne instruments to study the Arctic summer stratosphere (1997), where photolysis dominates the heterogenous reactions. Balloonborne experiments were used to examine the stratospheric chemistry during high aerosol load (1993) at northern midlatitudes [*Sen et al.*, 1998] and during different aerosol loads (1987–1997) at northern high and midlatitudes [*Jucks et al.*, 1999]. The Cryogenic Limb Array Etalon Spectrometer (CLAES: October 1991 to May 1993) and the Improved Stratospheric and Mesospheric Sounder (ISAMS: September 1991 to July 1992) [*Kumer et al.*, 1997] measured in the period of high volcanic aerosol load. *Danilin et al.* [1999] used these satellite data to study the global NO_y partitioning during the decline of the Mount Pinatubo aerosol load until September 1994. The global CRISTA measurements (November 1994 and August 1997) represent an important supplement to these previous data sets. They represent unique global N_2O_5 data sets under conditions of relatively low aerosol.

[10] Since CRISTA measures trace gases (e.g., NO_2, N_2O_5, $ClONO_2$, and HNO_3) via thermal emissions, it is independent of the solar zenith angle. Thus the measurements can be taken at all local times given by the orbit geometry. In addition, the simultaneous employment of three telescopes increases the local time range. Thus CRISTA data is especially suited to study the photochemistry and diurnal variations. The unprecedented high spatial resolution of the two global data sets provides the opportunity to investigate small-scale structures caused by transport and chemistry.

[11] Two-dimensional and spatially limited models (e.g., box models) have led to an improved quantitative understanding of NO_y chemistry, for example, concerning the compilations of reaction rates from the Jet Propulsion Laboratory (JPL) [*DeMore et al.*, 1994, 1997], hereinafter called JPL'94 and JPL'97. Comparisons with many measurements reveal [e.g., *Cohen et al.*, 2000; *Gao et al.*, 1997, 1999; *Osterman et al.*, 1999; *Jucks et al.*, 1999; *Sen et al.*, 1998] that models using JPL'97 rates underestimate NO_x/NO_y by up to 40%, but fit better to the measurements under higher aerosol conditions, when reaction (4) is not the dominant NO_x sink. The JPL'94 recommendations include a slower rate for reaction (4), leading to NO_x/NO_y values which are more consistent with measurements [e.g., *Osterman et al.*, 1999]. Updating the JPL'97 compilation with recent laboratory measurements [*Brown et al.*, 1999a, 1999b; *Dransfield et al.*, 1999; *Gierczak et al.*, 1999] of reactions (2), (4), and (5), as well as reducing the JPL'97 value of rate 4, increases the modeled NO_x/NO_y to more realistic values [e.g., *Cohen et al.*, 2000; *Kondo et al.*, 2000; *Osterman et al.*, 1999; *Jucks et al.*, 1999; *Danilin et al.*, 1999; *Randeniya et al.*, 1999]. *Brühl and Crutzen* [2000] pointed out that the importance of NO_x catalysis concerning stratospheric ozone loss is also enhanced when using the updates of the JPL'97 recommendations.

[12] Three-dimensional stratospheric models have been widely used to study both transport of long-lived tracers and chemistry and transport of chemically active species, e.g., the nitrogen family [e.g., *Lamarque et al.*, 1999; *Valks and Velders*, 1999; *Chipperfield*, 1999; *Khosravi et al.*, 1998; *Pierce et al.*, 1999; *Brasseur et al.*, 1997; *Kumer et al.*, 1997].

[13] Recently, assimilation has become more and more an application of three-dimensional models [e.g., *Khattatov et al.*, 2000; *Levelt et al.*, 1998]. Assimilation of chemically active species, such as the NO_y family, requires an accurate model representation of the diurnal cycle. By utilizing data of nitrogen, oxygen, and chlorine species from the Upper Atmosphere Research Satellite (UARS) *Khattatov et al.* [1999] demonstrated the value of assimilation techniques using irregular satellite data compared to common gridding and mapping methods, for synoptic analyses of photochemically short-lived species.

[14] In this paper the NO_y family members obtained during both CRISTA missions are assimilated into a CTM version of the National Center for Atmospheric Research (NCAR) Research for Ozone in the Stratosphere and its Evolution (ROSE) model [e.g., *Rose and Brasseur*, 1989; *Smith*, 1995]. First assimilation results of the CRISTA 1 mission were presented by *Riese et al.* [2000]. Here we discuss the second CRISTA mission and how it differs from the CRISTA 1 period. After a brief overview on the CRISTA experiment and data and the assimilation by means

of the ROSE model (section 2), the influence of medium-scale dynamics on NO_2 is demonstrated using CRISTA data (section 3). In section 4 the consistency of the CRISTA measurements of NO_y species with aerosol data from the Halogen Occultation Experiment (HALOE) [*Hervig et al.*, 1995, 1998] and SAGE II [*Thomason et al.*, 1997] is checked by means of the chemistry code included in the ROSE model. In section 5 measured diurnal cycles of N_2O_5 and NO_2 are analyzed and compared with the ROSE model. The differences in the diurnal cycles between the two CRISTA missions are discussed and the diurnal exchange between N_2O_5 and NO_2 is studied to directly check the chemical consistency of CRISTA data. CRISTA NO_2 measurements at or near the terminator are compared directly with HALOE observations [*Russell et al.*, 1993; *Gordley et al.*, 1996] of NO_x. In section 6 we estimate the effects of the changes in temperature and ozone between the two missions. The advantage of a simultaneously measured spatially highly resolved aerosol data set for the local representation of heterogenous chemistry is demonstrated for the CRISTA 1 period in section 7.

2. CRISTA Observations and Data Assimilation

[15] The limb scanning infrared experiment CRISTA was first flown in November 1994 during mission STS-66 [*Offermann et al.*, 1999] and for the second time in August 1997 during the NASA Space Shuttle mission STS-85 [*Grossmann et al.*, 2002]. From its orbit at 300 km altitude and 57° inclination, CRISTA collected spatially dense data sets (4–12 November 1994 and 8–16 August 1997) by means of three telescopes for simultaneous measurements and fast liquid helium cooled detectors. Spatial resolution at low and midlatitudes in the standard measuring modes is about 250 km along track and 600 km across track horizontally and 2 km vertically.

[16] Figure 1 shows typical latitudinal local time distributions of one day for both CRISTA missions. Each dot represents one height profile. During CRISTA 1, ascending orbit branches occurred during daytime and descending orbit branches in the night. During CRISTA 2, daytime measurements approximately correspond to the Northern Hemisphere and nighttime measurements to the Southern Hemisphere. The local time distributions shown in Figure 1 shift by 22 min per day toward earlier local times as the mission progresses. The three tracks of points (Figure 1, left side) correspond to the three telescopes, the employment of which extends the local time range at any given latitude to one to three hours.

[17] Since CRISTA is able to measure thermal emissions at all local times, the instrument is especially suited to observe the global diurnal cycle of chemically reactive species. The latitudinal local time distribution for CRISTA 2 (Figure 1, right side) exhibits some peculiarities as a result of several special measuring modes [*Grossmann et al.*, 2002].

[18] For both missions global distributions of a variety of trace gases were retrieved using an onion-peeling algorithm [*Riese et al.*, 1999a]. In the present paper CRISTA 1 version 4 data and CRISTA 2 version 1 data are presented. During both CRISTA missions over 95,000 profiles of several trace gases were collected. For CRISTA 2 mixing ratios of N_2O_5 and N_2O are only available from the two lateral telescopes [*Grossmann et al.*, 2002]. NO_2 mixing ratios, which are retrieved from emissions near 6.25 μm, show a very strong dependence on the assumptions concerning the background signal at altitudes where aerosol plays a significant role. For CRISTA 1 NO_2 data is only used down to a pressure level of 10 hPa, whereas for CRISTA 2 NO_2 could be retrieved down to about 22 hPa.

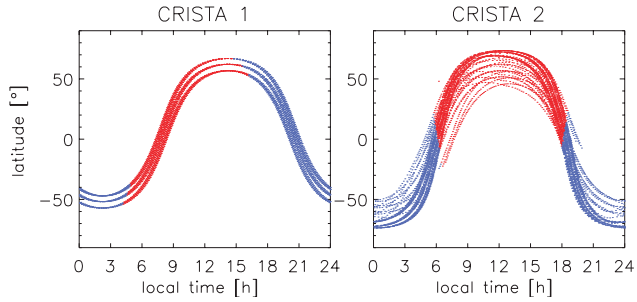

Figure 1. Latitudinal local time distribution on 9 November 1994 (CRISTA 1) and on 12 August 1997 (CRISTA 2) for all three telescopes. Red dots represent daytime measurements, and blue dots correspond to nighttime measurements.

[19] CRISTA measurements of O_3, which is important for NO_y gas phase chemistry, agree to 10% or better with several independent data sets [*Manney et al.*, 2001]. For HNO_3, CRISTA and Atmospheric Trace Molecule Spectroscopy (ATMOS) results generally agree to better than 15% [*Errera and Fonteyn*, 2001]. *Bacmeister et al.* [1999] compared CRISTA data including HNO_3 and O_3 with in situ measurements sampled by the ER-2 aircraft and found generally good agreement under meteorologically undisturbed conditions.

[20] CRISTA 1 and CRISTA 2 data are assimilated three-dimensionally into a CTM version of the ROSE model [*Riese et al.*, 1999b, 2000] employing a sequential assimilation scheme. The model is driven by wind and temperature fields provided by the UK Met Office (UKMO) [*Swinbank and O'Neill*, 1994]. The model grid comprises 72 points in latitude (≈300 km) and 64 points in longitude (≈400 km at midlatitudes). Thus the spatial resolution is similar to the measurement grid of CRISTA. In the vertical direction the model runs on a subset of the UARS standard pressure levels ($10^{\frac{i}{6}-\frac{1}{2}}$ hPa; i = 0, . . ., 18). The ROSE chemistry code uses the JPL'94 recommendations, with updated rates for reactions (2), (4), and (5) [*Brown et al.*, 1999a, 1999b; *Gierczak et al.*, 1999]. The CRISTA data is assimilated into the ROSE model following a family concept, which means that (besides the long-lived tracers N_2O, CH_4, CFC11) total family amounts of NO_y, Cl_y and O_x are inserted into the model. By means of the partitioning ratios of the photochemical model O_x is derived from ozone and Cl_y from $ClONO_2$. In the case of O_3 the modeled value is directly given by the measurement. The total NO_y family amount is estimated from HNO_3, N_2O_5, NO_2, and $ClONO_2$ separately using the partitioning ratios of the photochemical model. The resulting four independent NO_y estimates are error weighted and averaged [cf. *Riese et al.*, 2000] and the corresponding total NO_y is inserted into the ROSE model by the sequential assimilation scheme.

Thus the modeled NO_y partitioning is given by the model chemistry and the aerosol load. It is not constrained by the observed partitioning of the NO_y species.

[21] The model runs presented in this paper start on 1 November 1994 for the CRISTA 1 period and on 1 August 1997 for the CRISTA 2 period. The calculation of the initial trace gas fields is described by *Riese et al.* [1999b].

3. Dynamics and Photochemistry

[22] Due to its very dense spatial measurement grid CRISTA is able to resolve dynamical structures down to scales of about 200 km in its standard measurement modes. During both CRISTA missions, a variety of such structures were found, e.g., during CRISTA 1 three streamers of tropical air entering midlatitudes [e.g., *Offermann et al.*, 1999; *Riese et al.*, 1999b] were detected with widths ranging from over 1000 km down to the spatial resolution of the instrument.

[23] During CRISTA 2, a stratospheric streamer structure was found in the Southern Hemisphere, which was centered vertically at about 30 km altitude (≈10 hPa). *Riese et al.* [2002] show that the second CRISTA mission captured a period of extremely strong planetary wave activity in the Southern (winter) Hemisphere. These waves resulted in a large displacement of the southern polar vortex. The interaction of the vortex edge with the tropics led to an extraction of a planetary scale tongue of tropical air.

[24] *Riese et al.* [2000] showed maps of HNO_3, $ClONO_2$, and N_2O_5 for CRISTA 1. Here, we present for the first time horizontal distributions of NO_2 derived from CRISTA observations. Figure 2 shows CRISTA 2 measurements of N_2O and NO_2 at 10 hPa. For NO_2 the data from ascending orbit branches is shown (midnight to noon, cf. Figure 1).

[25] The measured N_2O field (Figure 2) reveals the streamer with tropical air rich in N_2O, which emerges from the tropics over the mid-Pacific, stretching across South America toward the tip of South Africa. Here the tropical air mass is split into two parts: one enters an anticyclone transporting the air mass back westward near the tropics, and the other is advected further southeastward. As discussed by *Riese et al.* [2002], the ROSE model captures the dynamical structures observed during CRISTA 2 very well.

[26] The high correlation between NO_y and N_2O (and other tracers) leads to dynamical structures in NO_2. The measured field of NO_2 (Figure 2) shows low mixing ratios over the South Atlantic (blue-green), which corresponds to the part of the streamer between the tip of South America and South Africa.

[27] The diurnal cycle in NO_2 leads to the dynamically induced structures being overlaid by a sharp decrease of NO_2 at the morning terminator at about 10°S and a slow increase to the northernmost point of the orbit, which roughly corresponds to local noon. Such streamers can transport tropical air masses very quickly and effectively to higher latitudes. Thus streamers may influence the NO_y partitioning at middle and higher latitudes by the injection of tropically partitioned NO_y.

4. Influence of Background Aerosol Data Sets

[28] Since total NO_y is assimilated in the ROSE model, the partitioning ratios of the modeled NO_y species only depend on the model chemistry. Thus the effect of the background aerosol on the model chemistry can be analyzed and compared to the observations.

[29] Two model runs were performed utilizing zonally averaged surface densities provided by the HALOE and SAGE II experiments as background aerosol data sets. Because of poor latitude coverage in the SAGE II data set for November 1994, data for October 1994 was used, which has similar values to the November data. Results of these two runs were interpolated onto the CRISTA measurement grid in space and local time. Both model results and measurements were zonally averaged for 10°-wide latitude bands and 1-hour local time windows. In Figures 3 and 4 resulting modeled and measured profiles of HNO_3, N_2O_5, and NO_2 from CRISTA 1 and CRISTA 2 are compared in two latitude bands (45–55°N and 35–45°S) for ascending orbit branches corresponding to morning measurements and descending orbit branches in the afternoon and evening (cf. latitudinal local time distribution in Figure 1). The model results mostly show remarkably good agreement with the measurements of the single nitrogen species.

[30] During CRISTA 1, especially at northern midlatitudes (Figure 3), results of the model run based on HALOE aerosol surface densities are slightly more consistent with the CRISTA data and the model chemistry than the run based on SAGE II aerosol data. This is because HALOE aerosol surface densities (November 1994) are somewhat higher than the SAGE II data both from November and October 1994.

[31] The modeled mixing ratios of HNO_3, which is the most abundant NO_y species in the lower stratosphere, are in good agreement with the observations. This is true even above about 15 hPa, where NO_2 dominates total NO_y. For CRISTA 1 data at northern midlatitudes the modeled NO_2 and N_2O_5 profiles mainly match the measurements within their error bars. At and above 6.8 hPa the model tends to underestimate measured NO_2 and N_2O_5. The reason for this may be a lack in our understanding of the photochemistry in this altitude region.

[32] CRISTA 2 data (Figure 4) is generally well reproduced by the model in both hemispheres. Due to the low solar zenith angles in the Northern Hemisphere (summer) N_2O_5 mixing ratios fall to very low values in the evening. Here the N_2O_5 retrieval runs near the detection limit (about 100 ppt as estimated from single profiles) resulting in large systematic N_2O_5 errors.

5. Changes in Diurnal Cycles and Aerosol

[33] Since the photolysis of N_2O_5 in the lower stratosphere is a depletion mechanism competing with heterogeneous conversion, the analysis of the influence of aerosol on the NO_y family members has to include the diurnal cycles as well. *Riese et al.* [2000] demonstrated the model's capability to reproduce CRISTA measurements properly for Northern Hemisphere evening conditions at higher altitudes (3.2 hPa and 10 hPa) during the CRISTA 1 mission. In this section the whole diurnal cycles in both hemispheres and also for lower altitudes is discussed and compared to the second CRISTA mission and measurements of the HALOE experiment.

[34] In Figures 5 and 6 the diurnal cycles of modeled NO_y family members (lines) and corresponding measurements (asterisks) are compared for two narrow latitude bands (45–

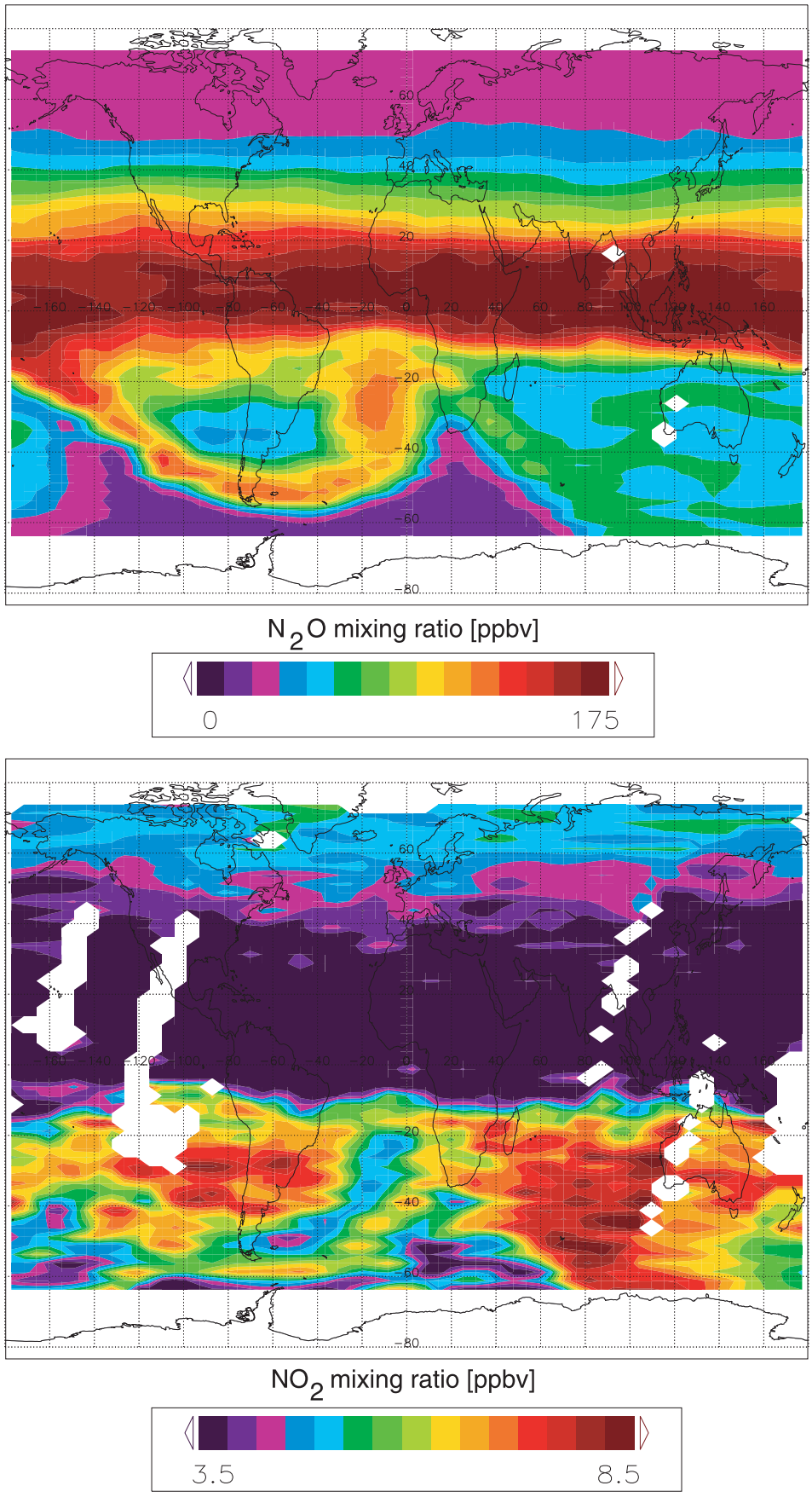

Figure 2. Horizontal structures in N_2O (upper map) and NO_2 (lower map) at 10 hPa (about 30 km altitude) on 12 August 1997 as measured by CRISTA 2. For details, see section 3.

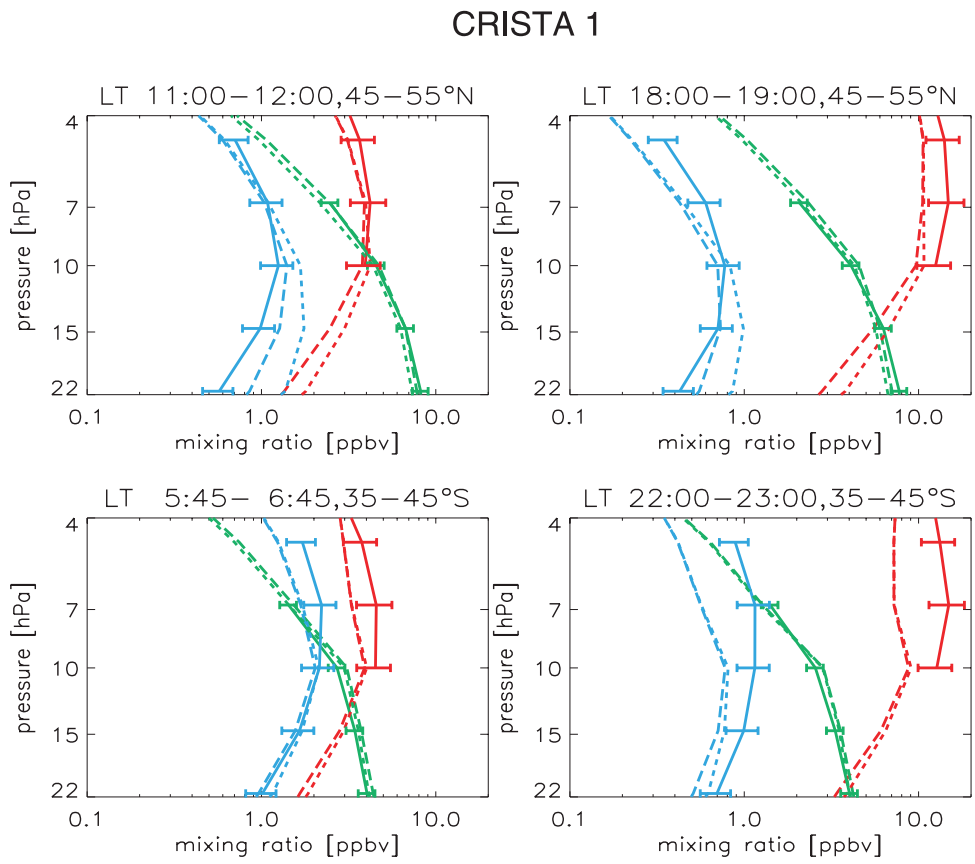

Figure 3. Intercomparison of CRISTA 1 measurements (solid curves) and ROSE assimilations (9 November 1994). Model results were obtained utilizing HALOE aerosol (long dashes) and SAGE II aerosol (short dashes). HNO_3 profiles are color coded in green, N_2O_5 in blue, and NO_2 in red. Zonal averages are shown for northern midlatitudes (45–55°N, upper row) and southern midlatitudes (35–45°S, lower row) at morning (left column) and afternoon local times (right column). Error bars denote systematic measurement errors.

55°N; 35–45°S). As Figure 5 shows, modeled values of HNO_3, N_2O_5, NO_2, and $ClONO_2$ agree well with the measurements. As expected, HNO_3, which has a photochemical lifetime of the order of days below 35 km [*Brasseur and Solomon*, 1986], shows practically no diurnal variations at 10 hPa and 22 hPa. Within the systematic error bars it is constant and is well reproduced by the model. The same holds for $ClONO_2$, which varies by up to 30% in the midlatitude measurements but also has much larger error bars, which include the large uncertainties in the $ClONO_2$ absorption cross sections (20%) [*Ballard et al.*, 1988] used for the retrieval.

[35] N_2O_5 shows significant diurnal variations in the measurements as well as in the model results, which agree within the systematic error bars. Also the temporal gradients are well captured by the model. At 22 hPa in the northern midlatitude band the modeled values are somewhat high compared to the measurements. In this situation, larger aerosol surface densities are more consistent with the CRISTA observations.

[36] At 10 hPa, especially across the terminators NO_2 measurements reveal large and steep variations with local time. This is well captured by the model. Since NO_2 equals NO_x during nighttime, CRISTA measurements and model results of NO_2 can directly be compared with HALOE measurements of NO_x (NO + NO_2). Since the NO_y chemistry is much slower than the NO_x chemistry (timescale of days versus minutes) [e.g., *Jucks et al.*, 1999; *Cohen et al.*, 2000], total NO_x is nearly constant across the terminator. Thus, concerning occultation measurements like HALOE, NO_x is better suited for comparisons than NO_2. Both modeled NO_x and CRISTA nighttime NO_2 agree well with HALOE NO_x (Figure 5, light blue diamonds), especially where HALOE errors [*Gordley et al.*, 1996] are small.

[37] In September 1988 *Webster et al.* [1990] measured diurnal variations of NO_2 with the Balloonborne Laser In Situ Sensor (BLISS). In order to compare with the BLISS measurements (32°N, 10–12 hPa), CRISTA 1 data is zonally averaged for 30–35°N, 10 hPa. NO_2, N_2O_5, and the other NO_y species measured by CRISTA are reproduced by the ROSE model well within the error bars in this latitude band. For the logarithmic slope of the night time decay of NO_2 derived from the BLISS measurements *Webster et al.* [1990] obtain $(-1.77 \pm 0.05) \times 10^{-5}s^{-1}$ ($T = 233$ K; O_3: 8.5 ppm, $2.747 \times 10^{12}cm^{-3}$). With CRISTA morning and evening measurements (and the modeled decrease of NO_2 at the morning terminator) a logarithmic slope of $(-1.1 \pm 0.2) \times 10^{-5}s^{-1}$ is obtained

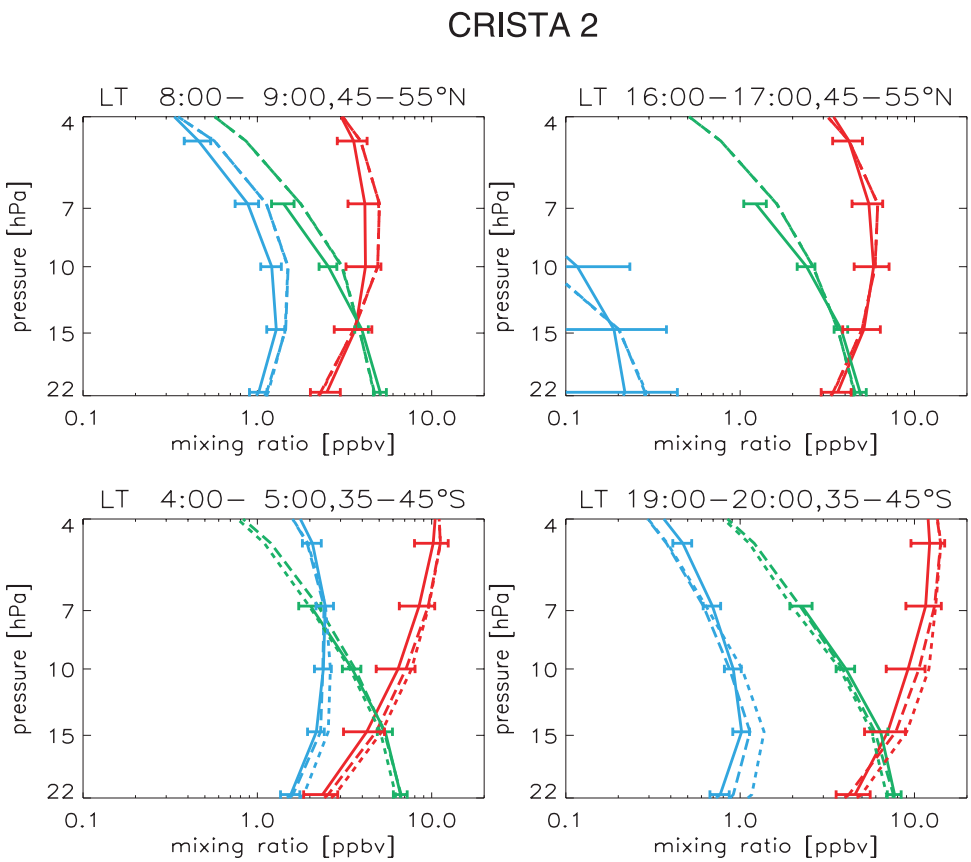

Figure 4. Same as Figure 3 but for CRISTA 2 (12 August 1997): In the 35–45°S latitude band only the longitude regions 100–0°W and 80–180°E were averaged to exclude the polar vortex and to avoid mixing of different air masses.

(T = 224 K; O_3: 7.3 ppm, 2.4×10^{12}cm^{-3}). The flatter slope of the night time decay of NO_2 in the case of CRISTA can be explained by a combined effect of lower temperature and lower ozone compared to the BLISS conditions as confirmed by the theoretical expected slope of $d/dt(ln\ [NO_2]) = -2\ k_6[O_3] = (-1.1 \pm 0.2) \times 10^{-5}s^{-1}$ for CRISTA.

[38] We now define the quantity $NO_x^{\#} = NO_x + 2\ N_2O_5$ both in order to summarize nitrogen oxides on the side of reactive nitrogen regarding the heterogeneous conversion to HNO_3 [*Brasseur and Granier*, 1992] and in order to take into account the exchange of NO_x with its nighttime reservoir N_2O_5. As can be seen from the modeled values, $NO_x^{\#}$ is nearly constant over the diurnal cycle (Figure 5). $NO_x^{\#}$ was also derived from CRISTA measurements of N_2O_5. For NO_x HALOE measurements were taken, because at 22 hPa NO_2 is not available during CRISTA 1. This combination of CRISTA and HALOE measurements (Figure 5, black diamonds) agrees well with the modeled $NO_x^{\#}$ values.

[39] Model results for CRISTA 2 (Figure 6) are of similar quality. In the southern latitude band, where HALOE measurements are available, HALOE NO_x agrees well with CRISTA nighttime measurements of NO_2. In addition, the model results of $NO_x^{\#}$ are in good agreement with values derived from HALOE NO_x and CRISTA N_2O_5. Compared to the first mission CRISTA 2 took place in nearly the opposite season. Thus diurnal variations of N_2O_5 at 10 hPa are now much more pronounced in the northern latitude band (summer). For both N_2O_5 and NO_2, which is also available at 22 hPa during CRISTA 2, absolute values and diurnal variations are well captured by the ROSE model.

[40] For CRISTA 2 the exchange between N_2O_5 and NO_2 can be checked directly from the measurements: during CRISTA 2 the morning and the evening terminator are located at almost the same latitude (near the equator, cf. Figure 1). Since NO_2 is partly converted to N_2O_5 during the night, the nighttime increase of N_2O_5 can be estimated from sunset and sunrise mixing ratios of NO_2 by the assumption that only reactions (6) and (7) have to be considered and other nighttime reservoirs of NO_x as e.g., HNO_3, $ClONO_2$, and NO_3 can be ignored [*Nevison et al.*, 1996]:

$$2\left([N_2O_5]_{SR} - [N_2O_5]_{SS}\right) = [NO_2]_{SS} - [NO_2]_{SR} \qquad (1)$$

[41] CRISTA 2 measurements of N_2O_5 and NO_2 zonally averaged in the latitude band of 5°S–15°N are used to validate equation (1). Since the tropics show little longitudinal variation, zonal averages can be used as representative values since for this direct comparison no dynamic effects are taken into account. As Figure 7 shows, the results from equation (1) agree well with the measurements within the error bars.

[42] Here in the middle tropical stratosphere, the other nighttime reservoirs all play a minor role: HNO_3 is low in the tropics, $ClONO_2$ becomes important in the lower strato-

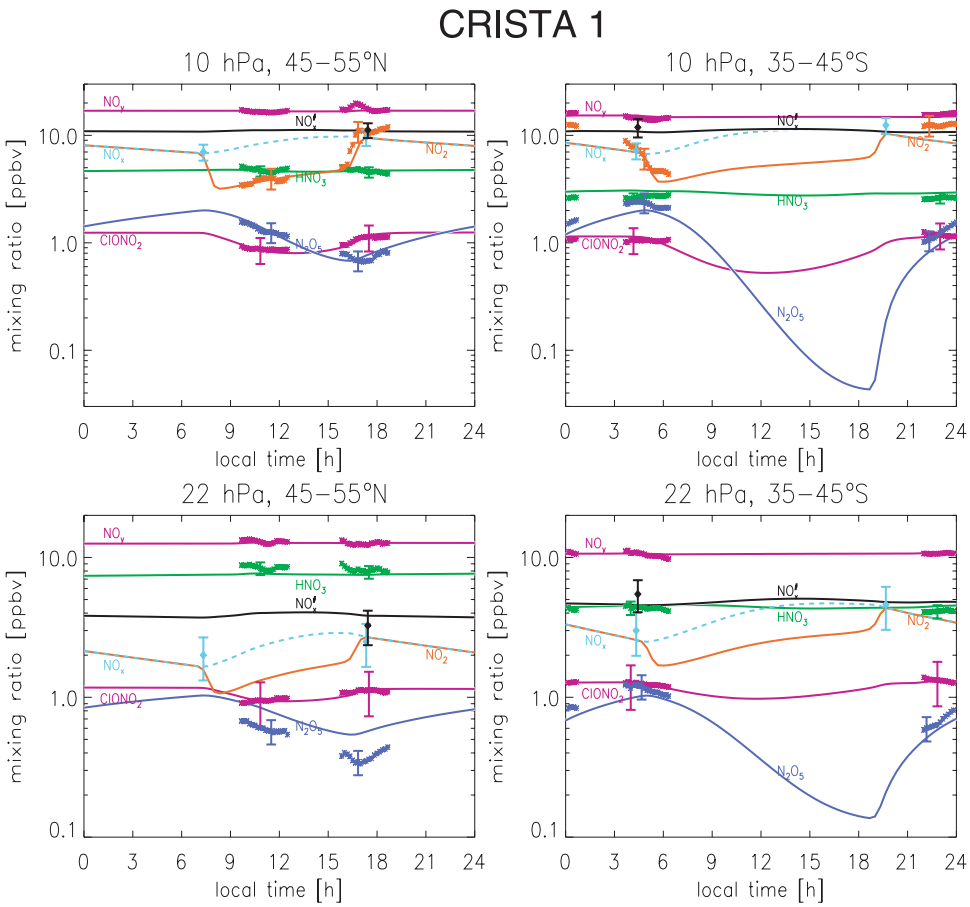

Figure 5. Intercomparison of CRISTA 1 measurements and modeled diurnal cycles (9 November 1994): CRISTA measurements with systematic error bars (green, orange, blue, and purple symbols) and modeled diurnal cycles (solid lines) of HNO_3, N_2O_5, NO_2, and $ClONO_2$ as well as (dashed line) NO_x distinct from NO_2 during the day. Black diamonds denote $NO_x^{\#}$ measurements derived from CRISTA N_2O_5 and HALOE NO_x. CRISTA measurements and modeled diurnal cycles were zonally averaged at northern midlatitudes (left column) and southern midlatitudes (right column) at 10 hPa (upper row) and 22 hPa (lower row). The measurements were averaged and binned in local time according to the model time steps of 20 min.

sphere and at higher latitudes, and NO_3 is generally about two orders of magnitude lower than NO_2 [e.g., *Renard et al.*, 1996; *Nevison et al.*, 1996]. Thus, considering the approximations leading to equation (1) and the systematic errors, CRISTA measurements of NO_2 and N_2O_5 are chemically consistent. This supports the assumption that $NO_x^{\#}$ is a temporally conserved quantity.

[43] Having demonstrated the robustness of $NO_x^{\#}$ against photolysis effects, measurements of $NO_x^{\#}$ and N_2O_5 are now used to analyze the aerosol effect on the NO_y chemistry. Measurements (instead of model results) are taken in order to obtain results independent of HALOE and SAGE aerosol data, which were used in the model runs. In the southern latitude band (35–45°S) we use $NO_x^{\#}$ combined from CRISTA and HALOE measurements. Since HALOE NO_x measurements are not available for most of the Northern Hemisphere during CRISTA 2, in the northern latitude band (45–55°N) instead of $NO_x^{\#}$, measurements of N_2O_5 from CRISTA are used.

[44] In the southern latitude band at 10 hPa $[NO_x^{\#}]/[NO_y]$ remains practically constant (0.80 ± 0.13 for CRISTA 1; 0.82 ± 0.12 for CRISTA 2). At 22 hPa $[NO_x^{\#}]/[NO_y]$ decreases slightly but not significantly (0.50 ± 0.13 for CRISTA 1; 0.31 ± 0.08 for CRISTA 2). Since during CRISTA 2 (winter) less NO_x and thus also less $NO_x^{\#}$ is produced by the photolysis of HNO_3, as a compensating effect less $NO_x^{\#}$ has to be converted back to HNO_3 to keep $[NO_x^{\#}]/[NO_y]$ constant. This is compatible with a further decreased aerosol load: in the southern latitude band (35–45°S) at 22 hPa SAGE aerosol only contains a slight decrease, which is not significant considering its uncertainty (30%, cf. *Thomason et al.* [1997]) but HALOE aerosol data shows a decrease from the first to the second CRISTA mission larger than its uncertainty (20%, cf. *Hervig et al.* [1998]).

[45] In the northern latitude band the analysis is based on N_2O_5 mixing ratios. Figure 8 shows measured zonally averaged N_2O_5 profiles (taken at or interpolated by means of modeled temporal gradients to sunrise) together with the corresponding model results for both CRISTA missions. In the northern latitude band at altitudes below 10 hPa measured N_2O_5 sunrise mixing ratios during CRISTA 2 are

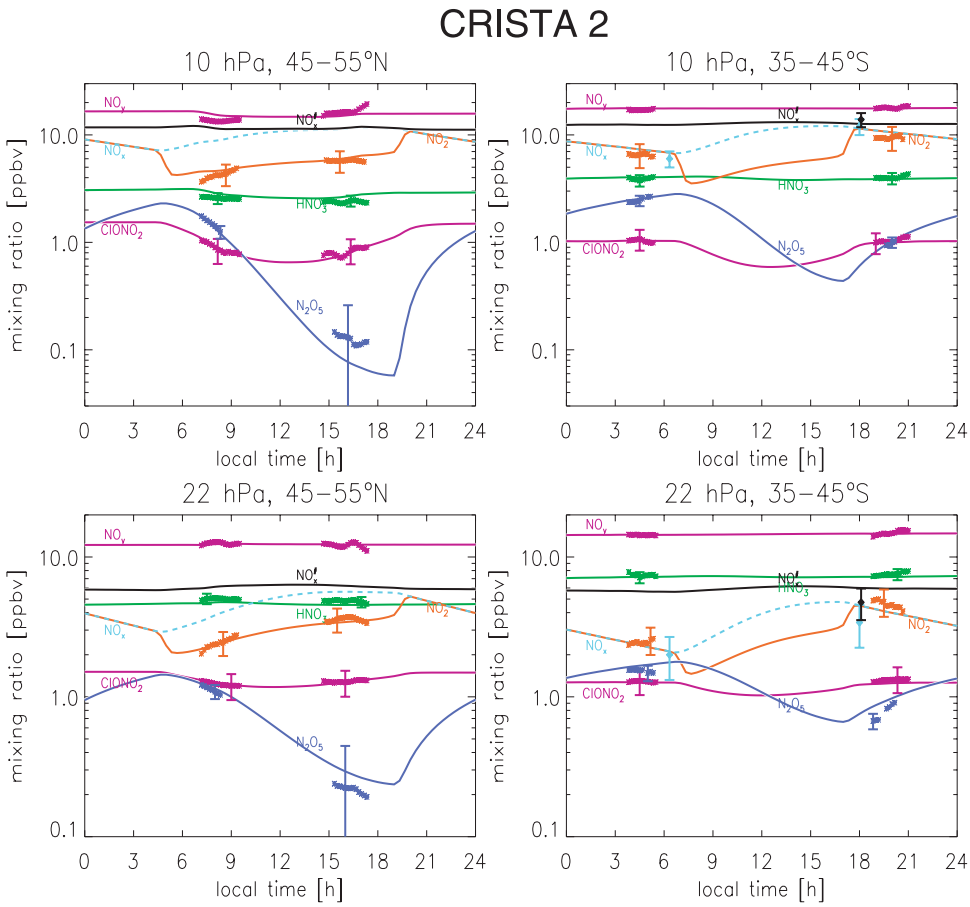

Figure 6. Same as Figure 5 but for CRISTA 2 (12 August 1997). In the 35–45°S latitude band only the longitude regions 100–0°W and 80–180°E were averaged to exclude the polar vortex and to avoid mixing of different air masses.

significantly higher (up to a factor 2 at 22 hPa) than during CRISTA 1. Total NO_y is similar for both missions at these altitudes (cf. Figures 5 and 6). Since from CRISTA 1 (northern winter) to CRISTA 2 (northern summer) photolysis increased, the increasing abundance of N_2O_5 is consistent with a lower aerosol load during CRISTA 2 at 22 hPa, 45–55°N, but may also be attributed to the stronger HNO_3 photolysis producing more NO_x during CRISTA 2. The model results of N_2O_5 mainly agree with the measurements considering the error bars, but are somewhat too high at 22 hPa during CRISTA 1. In the northern latitude band (45–55°N) both HALOE and SAGE aerosol decrease slightly but not significantly at 22 hPa between the two CRISTA missions. This is compatible with the findings from the analysis of CRISTA N_2O_5.

6. Dependence of N_2O_5 on Temperature and Ozone

[46] As discussed previously, N_2O_5 depends on the aerosol background and insolation. It also depends on temperature controlling the chemical reaction rates and on the gas-phase reactions with the dominant influence coming from ozone, which oxidizes NO_2 to N_2O_5 (reactions (6) and (7)).

[47] Since N_2O_5 mixing ratios during daytime are strongly seasonally dependent due to photolysis, mixing ratios at the morning maximum (sunrise) are compared (cf. section 5) for both CRISTA missions. The changes in measured N_2O_5 mixing ratios are derived directly from the CRISTA measurements at sunrise or by extrapolating the CRISTA morning measurements with the modeled temporal N_2O_5 gradients to

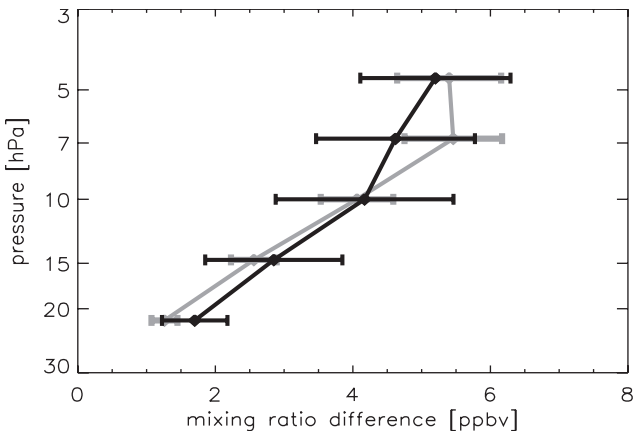

Figure 7. Vertical profiles of nighttime loss of NO_2 and nighttime production of N_2O_5 (cf. equation (1)). ΔNO_2 (black) and $2\Delta N_2O_5$ (grey) at 15°N–5°S for CRISTA 2 (12 August 1997).

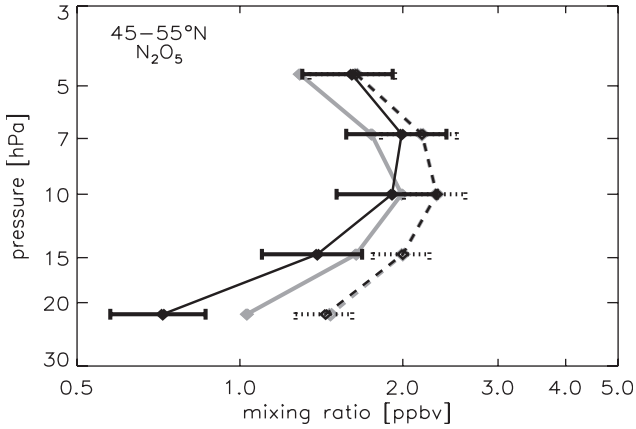

Figure 8. Vertical profiles of N_2O_5 taken at or interpolated to sunrise and zonally averaged for northern midlatitudes (45–55°N). Black curves and symbols correspond to CRISTA measurements and grey curves and symbols correspond to ROSE model results. Solid curves and full symbols represent results from the first mission and dashed curves and open symbols represent results from the second mission.

the local time of sunrise (cf. Figures 5 and 6). The results are summarized in Table 1.

[48] In order to estimate the changes in N_2O_5 mixing ratios due to ozone and temperature effects only, ROSE model runs were performed with varying ozone and temperature fields corresponding to the changes in UKMO temperatures and CRISTA ozone between the two CRISTA missions. The model results are shown in Table 1. The increase of N_2O_5 observed between CRISTA 1 and CRISTA 2 in the northern latitude band is much higher than the estimated upper limit for the increase due to temperature and ozone changes only. For the southern latitude band this difference is smaller.

[49] At 22 hPa the northern midlatitudes were dynamically undisturbed during CRISTA 2. During CRISTA 1 the northern latitude band contained two streamer structures [cf. *Riese et al.*, 2000], which also influenced N_2O_5 by transporting low mixing ratios toward midlatitudes. Thus the CRISTA 1 analysis shown in Table 1 was repeated excluding the longitude regions in the northern latitude band, which contained the streamer structures. But as the resulting values (Table 1, values in parentheses) show, this only causes a slight change in observed N_2O_5. The difference in ozone has only a small effect on N_2O_5 and the UKMO temperature field contains no streamer structures at all, as can also be confirmed by CRISTA 1 measurements.

[50] *Fish et al.* [2000], who studied NO_2 column density trends (1980–1998), stated that the influence of temperature, ozone, and water vapor on NO_2 is very small. Correspondingly it can be concluded from CRISTA measurements that the change in N_2O_5 due to ozone and temperature is much smaller than the observed change in N_2O_5.

[51] A trend in N_2O, which is the stratospheric source gas for NO_y chemistry, can be excluded as another factor influencing N_2O_5, because the trend in N_2O is less than about 3% per decade [*Fish et al.*, 2000]. Thus stratospheric aerosol remains as a dominant factor controlling N_2O_5 (except photolysis, e.g., of HNO_3 and N_2O_5).

7. Two Versus Three-Dimensionally Resolved Aerosol

[52] Usually even in three-dimensional models two-dimensional background aerosol fields are used. In standard applications the ROSE model utilizes zonally averaged aerosol surface densities, which are kept static during the whole model run. From the CRISTA retrievals also aerosol extinctions can be derived, which have the same high spatial resolution as the standard trace species data. This offers the opportunity to test the influence of small scale structures in the background aerosol on the chemistry. Here, the local effects of spatially highly resolved three-dimensional aerosol data versus zonally averaged two-dimensional aerosol data are investigated by means of two model cases for the first CRISTA mission.

[53] Model case 1 uses aerosol extinction data from CRISTA 1 converted into surface densities (Figure 9) following the method described by *Massie et al.* [1996]. The resulting aerosol fields were then normalized to the two-dimensional HALOE aerosol surface densities. The three-dimensional aerosol fields were assimilated into the ROSE model and advected by the transport scheme in the same manner as the trace gases. For model case 2, two-dimen-

Table 1. Observed and Modeled Differences in N_2O_5 Between the Two CRISTA Missions

Latitude Band	45–55°N	35–45°S
Observed N_2O_5 at sunrise (CRISTA 2)	1.44 ± 0.16 ppbv	1.64 ± 0.23 ppbv
Observed N_2O_5 at sunrise (CRISTA 1)	0.72 ± 0.14 ppbv (0.80 ± 0.15 ppbv)	1.22 ± 0.23 ppbv
Observed difference in N_2O_5	0.72 ± 0.21 ppbv (0.64 ± 0.21 ppbv)	0.42 ± 0.33 ppbv
Temperature difference	<13 K	<0 K
Estimated resulting difference in N_2O_5	<0.23 ppbv	<0.00 ppbv
Difference in ozone	<4% (8%)	<−2%
Estimated resulting difference in N_2O_5	<0.02 ppbv (0.03 ppbv)	<−0.02 ppbv
Estimated total temperature and ozone induced difference in N_2O_5	<0.25 ppbv (0.26 ppbv)	<−0.02 ppbv

Estimated differences in sunrise N_2O_5 at 22 hPa due to temperature and ozone differences between the two CRISTA periods and observed differences in N_2O_5. CRISTA 2 is compared with CRISTA 1. Values in parentheses were derived excluding the Northern Hemisphere streamer regions during CRISTA 1. For details see text.

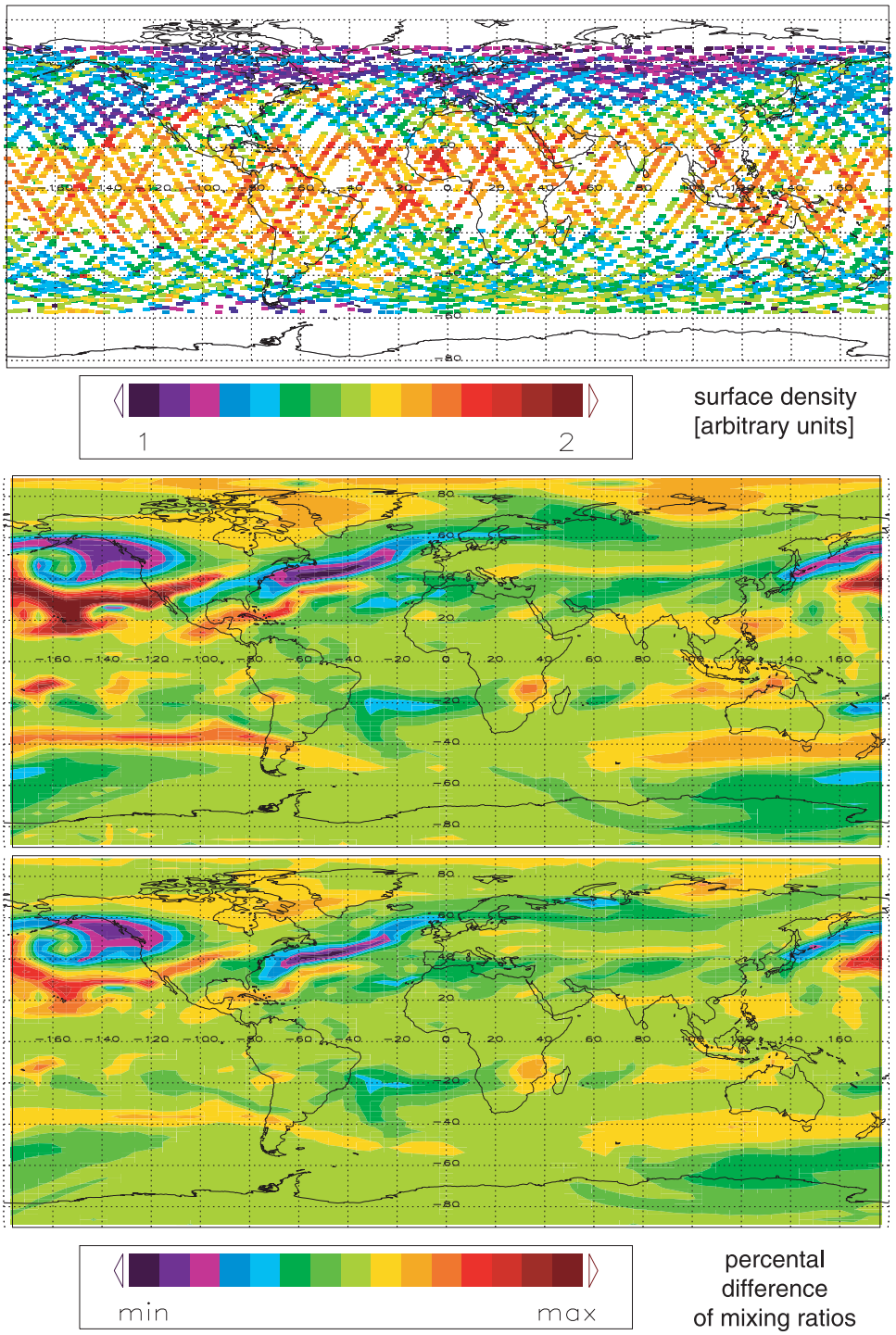

Figure 9. CRISTA 1 map of three-dimensionally resolved aerosol surface densities showing three streamers of tropical aerosol-enriched air across the United States and the Atlantic, over the east Asian coast, and across South America (upper map). Percental differences between a run with static two-dimensional aerosol from HALOE and fully assimilated and advected three-dimensional aerosol from CRISTA (normalized to HALOE) in modeled N_2O_5 (center map, color code from −30 to + 30%) and NO_2 fields (lower map, color code from −15 to + 15%). All maps are at 22 hPa (6 November 1994).

sional HALOE aerosol data was used and kept static during the trace gas assimilation. The resulting NO_2 and N_2O_5 distributions of both cases are compared in Figure 9.

[54] During CRISTA 1 three stratospheric streamers were found in inert tracer fields [*Offermann et al.*, 1999]. As shown in Figure 9, these streamers show up in aerosols as well: the North Atlantic streamer (stretching from southern California across the United States and the Atlantic toward Ireland), the North Asian streamer (from northern China across the Bering Sea to the northwestern Canadian Coast),

and the South American streamer (from Chile down to southwest of South Africa).

[55] As illustrated in Figure 9, the streamers in the aerosol field have a striking effect on N_2O_5 since its abundance is controlled by hydrolysis. Whereas most parts of the tropics and the Southern Hemisphere are obviously described in a good approximation by assuming a two-dimensional aerosol distribution, in the Northern Hemisphere, which is dynamically dominated by the two streamers, local differences in N_2O_5 between the two model cases are well above the statistical error for N_2O_5 (5% at 25 km altitude): the tropical aerosol-enriched air masses, which are transported in the streamers, reduce N_2O_5 about 30% more by hydrolysis than a zonally averaged aerosol background. NO_2 is somewhat less influenced by aerosols. As a result there are also areas where N_2O_5 is underestimated when using the two-dimensional aerosol field, for instance around the Aleutian high. Our sensitivity study highlights the importance of local structures in the aerosol field for the NO_y chemistry.

8. Conclusions

[56] During both missions CRISTA measured several key species of the NO_y family, such as HNO_3, N_2O_5, NO_2, and $ClONO_2$. The ROSE model, driven by UKMO wind and temperature analyses, was employed to assimilate estimates of total NO_y. Modeled NO_y species are in good agreement with corresponding CRISTA observations.

[57] During CRISTA 2, N_2O fields show a number of dynamical structures, such as a pronounced streamer in the Southern Hemisphere, transporting tropical air poleward, and a tongue of high-latitude air reaching to lower latitudes. Due to the high correlation between tracers (e.g., N_2O) and NO_y, in NO_2 fields these dynamical structures are detected as well.

[58] Employing updated NO_y reaction rates and background aerosol data from HALOE and SAGE II, NO_y species measured by CRISTA can be well modeled, with slightly better agreement when using HALOE aerosol data. The effect of heterogeneous chemistry on N_2O_5 and NO_2 becomes important below about 20 hPa and is also evident in HNO_3.

[59] Modeled diurnal variations of the NO_y family members, especially of the chemically active species N_2O_5 and NO_2, agree well with the measurements for both missions. Observations at or near the terminator show good agreement of CRISTA nighttime measurements of NO_2 and HALOE measurements of NO_x. For CRISTA 2 the diurnal conversion between NO_2 and N_2O_5 can be analyzed directly by means of the measurements. The nighttime NO_2 loss agrees well with the corresponding N_2O_5 increase, compatible with the role of N_2O_5 as an NO_2 nighttime reservoir. This confirms that $NO_x^{\#} = NO_x + 2\,N_2O_5$ is only weakly affected by photolysis. In the Southern Hemisphere $[NO_x^{\#}]/[NO_y]$ shows little variation from CRISTA 1 to CRISTA 2. In the Northern Hemisphere $[N_2O_5]$ as well as $[N_2O_5]/[NO_y]$ increase from the first to the second CRISTA mission. Model simulations show that the effect of temperature and ozone changes on N_2O_5 between the two CRISTA missions is small. Thus, if HNO_3 photolysis is taken into account, measured changes from CRISTA 1 to CRISTA 2 in N_2O_5 and $NO_x^{\#}$ are compatible with a decreased N_2O_5 hydrolysis in the Southern Hemisphere. In the Northern Hemisphere (summer) stronger HNO_3 photolysis competes with weaker N_2O_5 hydrolysis. This is compatible with the temporal development of aerosol as measured by SAGE II and HALOE during the two CRISTA missions. Thus N_2O_5 can be used as an indicator for the aerosol load, if changes due to photolysis are taken into account. As a more robust measure for the aerosol load, $NO_x^{\#}$ was introduced.

[60] Besides the large-scale evolution of aerosol, CRISTA measurements can also be used to quantify the effect of small-scale structures in background aerosol. It is shown that three-dimensional dynamical features (such as streamers) can alter modeled N_2O_5 values by about 30% compared to calculations based on a zonally symmetric aerosol distribution. The effect of streamers on NO_2 is about a factor of two smaller.

[61] **Acknowledgments.** We wish to acknowledge the support for the development of the CRISTA retrieval software and algorithms provided by L. L. Gordley and T. B. Marshall of Gordley Associated Software. We are also grateful to the HALOE and SAGE teams, who have provided their aerosol surface densities and NO_x (HALOE) via world wide web, as well as the UK Met Office for producing the meteorological data sets. The authors also wish to thank R. Spang for providing CRISTA 1 aerosol surface densities. The CRISTA experiments are funded by grant 50 OE 8503 and 50 QV 9501 of Deutsche Agentur für Raumfahrtangelegenheiten, Bonn, and Deutsches Zentrum für Luft- und Raumfahrt, Bonn. The work of X. Tie is supported by the DOE Atmospheric Chemistry Program under contract DE-AI05-94ER619577. The National Center for Atmospheric Research is sponsored by the National Science Foundation.

References

Bacmeister, J. T., V. Küll, D. Offermann, M. Riese, and J. W. Elkins, Intercomparison of satellite and aircraft observations of ozone, CFC-11, and NO_y using trajectory mapping, *J. Geophys. Res.*, *104*, 16,379–16,390, 1999.

Ballard, J., W. B. Johnson, M. R. Gunson, and P. T. Wassell, Absolute absorption coefficients of $ClONO_2$ infrared bands at stratospheric temperatures, *J. Geophys. Res.*, *93*, 1659–1665, 1988.

Bekki, S., and J. A. Pyle, A two-dimensional modeling study of the volcanic eruption of Mount Pinatubo, *J. Geophys. Res.*, *99*, 18,861–18,869, 1994.

Brasseur, G. P., and C. Granier, Mount Pinatubo aerosols, chlorofluorocarbons, and ozone depletion, *Science*, *257*, 1239–1242, 1992.

Brasseur, G. P., and S. Solomon, *Aeronomy of the Middle Atmosphere*, 2nd ed., 256 pp., D. Reidel, Norwell, Mass., 1986.

Brasseur, G. P., X. Tie, and P. J. Rasch, A three-dimensional simulation of the Antarctic ozone hole: Impact of anthropogenic chlorine on the lower stratosphere and upper troposphere, *J. Geophys. Res.*, *102*, 8909–8930, 1997.

Brown, S. S., R. K. Talukdar, and A. R. Ravishankara, Reconsideration of the rate constant for the reaction of hydroxyl radicals with nitric acid, *J. Phys. Chem. A*, *103*, 3031–3037, 1999a.

Brown, S. S., R. K. Talukdar, and A. R. Ravishankara, Rate constants for reaction $OH + NO_2 + M \rightarrow HNO_3$ under atmospheric conditions, *Chem. Phys. Lett.*, *299*, 277–284, 1999b.

Brühl, C., and P. J. Crutzen, NO_x-catalyzed destruction and NO_x activation at midlatitudes to high latitudes as the main cause of the spring to fall ozone decline in the Northern Hemisphere, *J. Geophys. Res.*, *105*, 12,163–12,168, 2000.

Chipperfield, M. P., Multiannual simulations with a three-dimensional chemical transport model, *J. Geophys. Res.*, *104*, 1781–1805, 1999.

Cohen, R. C., et al., Quantitative constraints on the atmospheric chemistry of nitrogen oxides: An analysis along chemical coordinates, *J. Geophys. Res.*, *105*, 24,283–24,304, 2000.

Crutzen, P. J., The influence of nitrogen oxides on the atmospheric ozone content, *Q. J. R. Meteorol. Soc.*, *96*, 320–325, 1970.

Danilin, M. Y., et al., Nitrogen species in the post-Pinatubo stratosphere: Model analysis utilizing UARS measurements, *J. Geophys. Res.*, *104*, 8247–8262, 1999.

Del Negro, L. A., et al., Comparison of modeled and observed values of NO_2 and $J(NO_2)$ during the Photochemistry of Ozone Loss in the Artic Region in Summer (POLARIS) mission, *J. Geophys. Res.*, *104*, 26,687–26,703, 1999.

DeMore, W. B., S. P. Sander, D. M. Golden, R. F. Hampson, M. J. Kurylo, C. J. Howard, A. R. Ravishankara, C. E. Kolb, and M. J. Molina, Chemical kinetics and photochemical data for use in stratospheric modeling, *JPL Publ.*, *94–26*, 1994.

DeMore, W. B., S. P. Sander, D. M. Golden, R. F. Hampson, M. J. Kurylo, C. J. Howard, A. R. Ravishankara, C. E. Kolb, and M. J. Molina, Chemical kinetics and photochemical data for use in stratospheric modeling, *JPL Publ.*, *97–4*, 1997.

Dransfield, T. K., K. K. Perkins, N. M. Donahue, J. G. Anderson, M. M. Sprengnether, and K. L. Demerjian, Temperature and pressure dependent kinetics of the gas-phase reaction of the hydroxyl radical with nitrogen dioxide, *Geophys. Res. Lett.*, *26*, 687–690, 1999.

Errera, Q., and D. Fonteyn, Four-dimensional variational chemical assimilation of CRISTA stratospheric measurements, *J. Geophys. Res.*, *106*, 12,253–12,265, 2001.

Fahey, D. W., et al., In situ measurements constraining the role of sulphate aerosols in midlatitude ozone depletion, *Nature*, *363*, 509–514, 1993.

Fish, D. J., H. K. Roscoe, and P. V. Johnston, Possible causes of stratospheric NO_2 trends observed at Lauder, New Zealand, *Geophys. Res. Lett.*, *27*, 3313–3316, 2000.

Gao, R. S., et al., Partitioning of the reactive nitrogen reservoir in the lower stratosphere of the Southern Hemisphere: Observations and modeling, *J. Geophys. Res.*, *102*, 3935–3949, 1997.

Gao, R. S., et al., A comparison of observations and model simulations of NO_x, NO_y in the lower stratosphere, *Geophys. Res. Lett.*, *26*, 1153–1156, 1999.

Gierczak, T., J. B. Burkholder, and A. R. Ravishankara, Temperature dependent rate for the reaction $O(^3P) + NO_2 \rightarrow NO + O_2$, *J. Phys. Chem. A*, *103*, 877–883, 1999.

Gordley, L. L., et al., Validation of nitric oxide and nitrogen dioxide measurements made by the Halogen Occultation Experiment for UARS platform, *J. Geophys. Res.*, *101*, 10,241–10,266, 1996.

Grossmann, K.-U., D. Offerman, O. Gusev, J. Oberheide, M. Riese, and R. Spang, The CRISTA 2 mission, *J. Geophys. Res.*, *107*, 10.1029/2001JD000667, in press, 2002.

Hervig, M. E., J. M. Russell III, L. L. Gordley, J. Daniels, S. R. Drayson, and J. H. Park, Aerosol effects and corrections in the Halogen Occultation Experiment, *J. Geophys. Res.*, *100*, 1067–1079, 1995.

Hervig, M. E., T. Deshler, and J. M. Russell III, Aerosol size distributions obtained from HALOE spectral extinction measurements, *J. Geophys. Res.*, *103*, 1573–1583, 1998.

Johnston, H., Reduction of stratospheric ozone by nitrogen oxide catalysts from supersonic transport exhaust, *Science*, *173*, 517–522, 1971.

Jucks, K. W., D. G. Johnston, K. V. Chance, W. A. Traub, and R. J. Salawitch, Nitric acid in the middle stratosphere as a function of altitude and aerosol loading, *J. Geophys. Res.*, *104*, 26,715–26,723, 1999.

Khattatov, B. V., J. C. Gille, L. V. Lyjak, G. P. Brasseur, V. L. Dvortsov, A. E. Roche, and J. W. Waters, Assimilation of photochemically active species and analysis of UARS data, *J. Geophys. Res.*, *104*, 18,715–18,737, 1999.

Khattatov, B. V., J.-F. Lamarque, L. V. Lyjak, R. Menard, P. Levelt, X. Tie, G. P. Brasseur, and J. C. Gille, Assimilation of satellite observations of long-lived chemical species in global chemistry transport models, *J. Geophys. Res.*, *105*, 29,135–29,144, 2000.

Khosravi, R., G. P. Brasseur, A. K. Smith, D. W. Rush, J. W. Waters, and J. M. Russel III, Significant reduction in the stratospheric ozone deficit using a three-dimensional model constrained with UARS data, *J. Geophys. Res.*, *103*, 16,203–16,219, 1998.

Kinnison, D. E., K. E. Grant, P. S. Connell, D. A. Rotman, and D. J. Wuebbles, The chemical and radiative effects of the Mount Pinatubo eruption, *J. Geophys. Res.*, *99*, 25,705–25,731, 1994.

Koike, M., N. B. Jones, W. A. Matthews, P. V. Johnston, R. L. McKenzie, D. Kinnison, and J. Rodriguez, Impact of Pinatubo aerosols on the partitioning between NO_2 and HNO_3, *Geophys. Res. Lett.*, *21*, 597–600, 1994.

Kondo, Y., T. Sugita, M. Koike, S. R. Kawa, M. Y. Danilin, J. M. Rodriguez, S. Spreng, K. Golinger, and F. Arnold, Partitioning of reactive nitrogen in the midlatitude lower stratosphere, *Geophys. Res. Lett.*, *105*, 1417–1424, 2000.

Kumer, J. B., S. R. Kawa, A. E. Roche, J. L. Mergenthaler, S. E. Smith, F. W. Taylor, P. S. Connell, and A. R. Douglass, UARS first global N_2O_5 data sets: Application to a stratospheric warming event in January 1992, *J. Geophys. Res.*, *102*, 3575–3582, 1997.

Lamarque, B. V., P. G. Hess, and X. Tie, Three-dimensional model study of the influence of stratosphere-troposphere exchange and its distribution on tropospheric chemistry, *J. Geophys. Res.*, *104*, 26,363–26,372, 1999.

Levelt, P. F., B. V. Khattatov, J. C. Gille, G. P. Brasseur, X. Tie, and J. W. Waters, Assimilation of MLS ozone measurements in the global three-dimensional chemistry transport model ROSE, *Geophys. Res. Lett.*, *25*, 4493–4496, 1998.

Manney, G. L., Comparison of satellite ozone observations in coincident air masses in early November 1994, *J. Geophys. Res*, *106*, 9923–9943, 1994.

Massie, S. T., T. Deshler, G. E. Thomas, J. L. Mergenthaler, and J. M. Russel III, Evolution of the infrared properties of the Mount Pinatubo aerosol cloud over Laramie, Wyoming, *J. Geophys. Res.*, *101*, 23,007–23,019, 1996.

McCormick, P. M., W. L. Thomason, and C. R. Trepte, Atmospheric effects of the Mt. Pinatubo eruption, *Nature*, *373*, 399–404, 1995.

Morris, G. A., D. B. Considine, A. E. Dessler, S. R. Kawa, J. Kumer, J. Mergenthaler, A. Roche, and J. M. Russel III, Nitrogen partitioning in the middle stratosphere as observed by the Upper Atmosphere Research Satellite, *J. Geophys. Res.*, *102*, 8955–8965, 1997.

Nevison, C. D., S. Solomon, and J. M. Russell III, Nighttime formation of N_2O_5 inferred from the Halogen Occultation Experiment sunset/sunrise NO_x ratios, *J. Geophys. Res.*, *104*, 6741–6748, 1996.

Offermann, D., K. U. Grossmann, P. Barthol, P. Knieling, M. Riese, and R. Trant, Cryogenic Infrared Spectrometers and Telescopes for the Atmosphere (CRISTA) experiment and middle atmosphere variability, *J. Geophys. Res.*, *104*, 16,311–16,325, 1999.

Osterman, G. B., B. Sen, G. C. Toon, R. J. Salawitch, J.-F. Margitan, J. J. Blavier, D. W. Fahey, and R. S. Gao, Partitioning of NO_y species in the summer Arctic stratosphere, *Geophys. Res. Lett.*, *26*, 1157–1160, 1999.

Perkins, K. K., et al., The NO_x-HNO_3 system in the lower stratosphere: Insights from in situ measurements and implications of the J_{HNO3}-[OH] relationship, *J. Phys. Chem. A*, *105*, 1521–1534, 2001.

Pierce, R. B., J. A. Al-Saadi, T. D. Fairlie, J. R. Olsen, R. S. Eckman, W. L. Grose, G. S. Lingenfelser, and J. M. Russell III, Large-scale stratospheric ozone photochemistry and transport during the POLARIS Campaign, *J. Geophys. Res.*, *104*, 26,525–26,545, 1999.

Portmann, R. W., S. S. Brown, T. Gierczak, R. K. Talukdar, J. B. Burkholder, and A. R. Ravishankara, Role of nitrogen oxides in the stratosphere: A reevaluation based on laboratory studies, *Geophys. Res. Lett.*, *26*, 2387–2390, 1999.

Randel, J. W., F. Wu, J. M. Russell III, and J. W. Waters, Space-time pattern of trends in stratospheric constituents derived from UARS measurements, *J. Geophys. Res.*, *104*, 3711–3727, 1999.

Randeniya, L. K., I. C. Plumb, and K. R. Ryan, NO_y and Cl_y partitioning in the middle stratosphere: A box model investigation using HALOE data, *J. Geophys. Res.*, *104*, 26,667–26,686, 1999.

Renard, J.-B., M. Pirre, C. Roberts, G. Moreau, D. Huguenin, and J. M. Russell III, Nocturnal vertical distribution of stratospheric O_3, NO_2 and NO_3 from balloon measurements, *J. Geophys. Res.*, *101*, 28,793–28,804, 1996.

Riese, M., R. Spang, P. Preusse, M. Ern, M. Jarisch, D. Offermann, and K. U. Grossmann, Cryogenic Infrared Spectrometers and Telescopes for the Atmosphere (CRISTA) data processing and atmospheric temperature and trace gas retrieval, *J. Geophys. Res.*, *104*, 16,349–16,367, 1999a.

Riese, M., X. Tie, G. P. Brasseur, and D. Offermann, Three-dimensional simulations of stratospheric trace gas distributions measured by CRISTA, *J. Geophys. Res.*, *104*, 16,419–16,435, 1999b.

Riese, M., V. Küll, X. Tie, G. P. Brasseur, D. Offermann, G. Lehmacher, and A. Franzen, Modeling of nitrogen species measured by CRISTA, *Geophys. Res. Lett.*, *27*, 2221–2224, 2000.

Riese, M., G. L. Manney, J. Oberheide, X. Tie, R. Spang, and V. Küll, Stratospheric transport by planetary wave mixing as observed during CRISTA 2, *J. Geophys. Res.*, *107*, 8179, 10.1029/2001JD000629, 2002.

Rinsland, C. P., M. R. Gunson, M. C. Abrams, L. L. Lowes, R. Zander, E. Mahieu, A. Goldman, M. K. W. Ko, J. M. Rodriguez, and N. D. Sze, Heterogeneous conversion of N_2O_5 to HNO_3 in the post Mount Pinatubo eruption stratosphere, *J. Geophys. Res.*, *99*, 8213–8219, 1994.

Rose, K., and G. P. Brasseur, A three-dimensional model of chemically active trace species in the middle atmosphere during disturbed winter conditions, *J. Geophys. Res.*, *96*, 16,387–16,403, 1989.

Russell, J. M., III, L. L. Gordley, J. H. Park, S. R. Drayson, W. D. Hesketh, R. J. Cicerone, A. F. Tuck, J. E. Frederick, J. E. Harries, and P. J. Crutzen, The Halogen Occultation Experiment, *J. Geophys. Res.*, *98*, 10,777–10,797, 1993.

Sen, B., G. C. Toon, G. B. Osterman, J.-F. Blavier, J. J. Margitan, and R. J. Salawitch, Measurements of reactive nitrogen in the stratosphere, *J. Geophys. Res.*, *103*, 3571–3585, 1998.

Smith, A. K., Numerical simulation of global variations of temperature, ozone, and trace species in the stratosphere, *J. Geophys. Res.*, *100*, 1253–1269, 1995.

Swinbank, R., and A. O'Neill, A stratosphere-troposphere data assimilation system, *Mon. Weather Rev.*, *82*, 686–702, 1994.

Thomason, L. W., L. R. Poole, and T. Deshler, A global climatology of stratospheric aerosol surface area density deduced from Stratospheric Aerosol and Gas Experiment II measurements: 1984–1994, *J. Geophys. Res.*, *102*, 8967–8976, 1997.

Tie, X., G. P. Brasseur, B. Briegleb, and C. Granier, Two-dimensional simulation of Pinatubo aerosol and its effect on stratospheric ozone, *J. Geophys. Res.*, *99*, 20,545–20,562, 1994.

Valks, P. J. M., and G. J. M. Velders, The present-day and future impact of NO_x emissions from subsonic aircraft on the atmosphere in relations to the impact of NO_x surface sources, *Ann. Geophys.*, *17*, 1064–1079, 1999.

Webster, C. R., R. D. May, R. Toumi, and J. A. Pyle, Active nitrogen partitioning and the nighttime formation of N_2O_5 in the stratosphere: Simultaneous in situ measurements of NO, NO_2, HNO_3, O_3, and N_2O using the BLISS diode laser spectrometer, *J. Geophys. Res.*, *95*, 13,851–13,866, 1990.

Webster, C. R., R. D. May, M. Allen, L. Jaegle, and M. P. McCormick, Balloon profiles of stratospheric NO_2 and HNO_3 for testing the heterogeneous hydrolysis of N_2O_5 on sulfate aerosols, *Geophys. Res. Lett.*, *21*, 53–56, 1994.

G. P. Brasseur, Max Planck Institute for Meteorology, Bundesstr. 55, D-20146 Hamburg, Germany. (Brasseur@dkrz.de)

G. Eidmann, Vacuumschmelze GmbH & Co. KG, Grüner Weg 37, D-63450 Hanau, Germany. (Gunnar.Eidmann@Vacuumschmelze.com)

V. Küll and D. Offermann, Physics Department, University of Wuppertal, Gaussstr. 20, D-42097 Wuppertal, Germany. (kuell@wpos2.physik.uni-wuppertal.de; offerm@wpos2.physik.uni-wuppertal.de)

M. Riese, Institute for Stratospheric Research, Juelich Research Center, D-52425 Juelich, Germany. (m.riese@fz-juelich.de)

X. Tie, National Center for Atmospheric Research, P.O. Box 3000, Boulder, CO 80307-3000, USA. (xxtie@acd.ucar.edu)

T. Wiemert, T-Systems GEI GmbH, Box 500144, D-52085 Aachen, Germany. (thomas.wiemert@t-systems.com)